Carcinogenesis vol.32 no.4 pp.452–461, 2011
doi:10.1093/carcin/bgq273
Advance Access publication December 22, 2010

IRIZIO: a novel gene cooperating with PAX3-FOXO1 in alveolar rhabdomyosarcoma (ARMS)

Fabrizio Picchione, Colin Pritchard[1], Irina Lagutina, Laura Janke and Gerard C.Grosveld*

Department of Genetics and Tumor Cell Biology, St Jude Children's Research Hospital, 262 Danny Thomas Place, Memphis, TN 38105, USA

[1]Present address: Division of Molecular Genetics, Netherlands Cancer Institute, Plesmanlaan 121, 1066 CX, Amsterdam, The Netherlands

*To whom correspondence should be addressed. Tel: +1 901 595 2279; Fax: +1 901 595 6035;
Email: gerard.grosveld@stjude.org

Rhabdomyosarcoma (RMS) is the most common soft-tissue sarcoma in children with an annual incidence of five new cases per million. Alveolar rhabdomyosarcoma (ARMS) is characterized by the t(2;13) or t(1;13) chromosomal translocations, which generate the *PAX3-FOXO1* or *PAX7-FOXO1* fusion genes, respectively. The oncogenic activity of *PAX3-FOXO1* has been demonstrated *in vitro* and *in vivo*, yet expression of the fusion protein alone in primary myoblasts or a mouse model is insufficient for tumorigenic transformation. To identify genes cooperating with *PAX3-FOXO1* in ARMS tumorigenesis, we generated a retroviral complementary DNA (cDNA) expression library from the Rh30 ARMS cell line. *Arf−/−* myoblasts expressing PAX3-FOXO1 and the retroviral cDNA library rapidly formed tumors after subcutaneous injection into NOD–SCID mice. Tumors formed by *Arf−/−/PAX3-FOXO1/* MarX-library myoblasts contained an unknown cDNA, encoding the C-terminus of the *Homo sapiens* hypothetical protein, FLJ10404, herein named IRIZIO. Expression of full length *IRIZIO* cDNA also cooperated with PAX3-FOXO1 in the transformation of *Arf−/−* myoblasts. Given that IRIZIO is expressed at increased levels in RMS, it might contribute to rhabdomyosarcomagenesis in humans.

Introduction

Rhabdomyosarcomas (RMS) are fast-growing malignant tumors, which account for over half of the soft tissue sarcomas in children (1). RMS is divided into two major histological subtypes, alveolar rhabdomyosarcoma (ARMS) and embryonal rhabdomyosarcoma (ERMS). ARMS may arise from immature skeletal muscle cells that remain partially differentiated, grow in alveoli-like structures and typically affects adolescents. While ERMS does not show any consistent and unique genetic alterations, ARMS is characterized by chromosomal translocations fusing the *PAX3* [t(2;13)] or *PAX7* [t(1;13)] gene to *FKHR* (*FOXO1*) (2). The *PAX3-FOXO1* gene plays a key role in 55–75% of ARMS, whereas the *PAX7-FOXO1* fusion gene is present in the remaining 10–22% of cases (3). The PAX3-FOXO1 protein possesses greater transcriptional activity than wild-type PAX3 protein (4), which plays a role during embryonic myogenesis (5). The presence of PAX3-FOXO1 might initiate a deregulated muscle developmental program in affected cells. Moreover, PAX3-FOXO1 has been linked to increased incidence of metastases and unfavorable outcome (3). Despite its oncogenic activity (6,7), *PAX3-FOXO1* requires additional genetic events to cause ARMS (8,9). Disruption of the pRb and p53 pathways are implicated in ARMS tumorigenesis in humans and mice (10–13). Our experiments demonstrate that PAX3-FOXO1 in combination with a defective p53 pathway (*Arf−/−*) alone is insufficient to transform primary mouse myoblasts and needs a compromised pRB pathway for full transformation. Using an expression complementary DNA (cDNA) library from an ARMS cell line, we identified a gene that cooperates in the tumorigenic transformation of *PAX3-FOXO1*-expressing *Arf−/−* myoblasts. This gene, *IRIZIO*, is upregulated in ARMS and may therefore contribute to rhabdomyosarcomagenesis in humans.

Abbreviations: ARMS, alveolar rhabdomyosarcoma; BSA, bovine serum albumin; cDNA, complementary DNA; DAB, 3,3′diaminobenzidine; ERMS, embryonal rhabdomyosarcoma; HA, hemagglutinin; NES, nuclear export signal; ORF, open reading frame; PCR, polymerase chain reaction; RMS; rhabdomyosarcoma.

Materials and methods

Constructs

The MARX vector was a gift from Dr David Beach. *IRIZIO* (FLJ10404) *Δ7* and *Δ7/8* cDNA were cloned into the MSCV-I-GFP vector using standard cloning techniques: the 5′ half of the cDNA sequence was excised from the plasmid pOBT-FLJ10404 (Open Biosystems, Thermo Fisher Scientific, Waltham, MA), starting from the unique StuI restriction site present in exon 9; the rest of the splice-specific sequences were polymerase chain reaction (PCR)-amplified from cDNA prepared from the ARMS cell line RH2, using primers specific for the region upstream of the StuI site. PCR fragments were generated with Phusion High-Fidelity PCR Kit (Finnzymes; Fisher Scientific, Pittsburgh, PA) using the following primers: forward 5′-ATGCCAAAGCTC-GTCAAGAATC-3′ and reverse 5′-GGCTGCTCAGGAAGCTGTTGAC-3′. Plasmids pSM2-Non-Targeting shRNA and IRIZIO-specific shRNA were purchased from Open Biosystems.

Generation of the ARMS cDNA library and its use in an in vivo complementation transformation screen

We generated a cDNA expression library from the RH30 ARMS poly(A)+ RNA in a MarX retroviral vector modified by the introduction of two SfiI sites harboring dissimilar internal sequences allowing directional cloning of the cDNAs (Figure 1) using a BD Biosciences smart kit for the synthesis of full-length cDNA (complexity = 2×10^7 clones). Freshly isolated p*16/Arf−/−* myoblasts (passage 4) were transduced with MSCV-SV40-Puro, MSCV-*PAX3*-SV40-Puro or MSCV-*PAX3-FOXO1*-SV40-Puro retroviruses and selected with 1.5 μg ml^{-1}puromycin (Sigma, St Louis, MO). Cells (2×10^4) were plated in soft agar in 6 cm dishes and colonies were scored 12–14 days later. *Arf−/−* mouse primary myoblasts expressing MSCV-SV40-Puro, MSCV-*PAX3*-SV40-Puro and MSCV-*PAX3-FOXO1*-SV40-Puro were transduced with the RH30 MarX-cDNA library and 48 h after transduction, plates were split 1:2 and cultured in the presence of 200 μg ml^{-1} hygromycin B (50 mg/ml; Cellgro, Manassas, VA) for 7–9 days. Hygromycin B resistant myoblasts (2×10^6) from each pool were subcutaneously injected into the hind and fore right flanks of NOD/SCID mice. cDNA inserts were PCR amplified from tumor genomic DNA with oligonucleotide primers flanking the SfiI sites in the MarX vector (forward primer: 5′-TTTATCCAGCCCTCACTCC-3′ and reverse primer: 5′-CGCTCACAATTCCACACTC-3′). Inserts were identified by DNA sequence analysis.

Isolation of mouse primary myoblast and tumor cells

Primary myoblasts were isolated from 1- to 3-day-old *Arf−/−* or wild-type littermates as described previously (14). Myoblasts were cultured in Ham's F10 medium supplemented with 20% of Cosmic Calf Serum (Hyclone, Logan, UT), human basic fibroblasts growth factor 1 ng/ml (Promega, Madison, WI), penicillin/streptomycin (100 μ/ml and 100 μg/ml, respectively) (Gibco-Invitrogen Corporation, Grand Island, NY) and plated on gelatin coated dishes at 37°C, 5% CO_2 and 6% O_2.

Tumor bearing mice were sacrificed using carbon dioxide asphyxiation and tumors were excised using sterile scissors. Tumor cells were isolated in the same way we isolate myoblasts (14). Part of the tumor cell suspension was used for genomic DNA isolation and the rest was cultured.

Cell culture, retroviral transduction and DNA transfection

ERMS (RD, JR1, RH6 and RH2), ARMS (RH30, RH4, RH41 RH3 and RH28) and 293T (human embryonic kidney) cells lines were grown in Dulbecco's Modified Eagle's Medium, 10% Cosmic Serum (Hyclone) and penicillin/streptomycin (100 μ/ml and 100 μg/ml, respectively; Gibco-Invitrogen Corporation). Human myoblasts (Lonza, Allendale, NJ) were cultured following the supplier's protocol. Retrovirus supernatants were generated by transfecting 293T cells using calcium phosphate as described previously (15). GFP+ cells were sorted by fluorescence activated cell sorting 48 h after transduction or were selected chemically depending on the selectable marker. Puromycin at

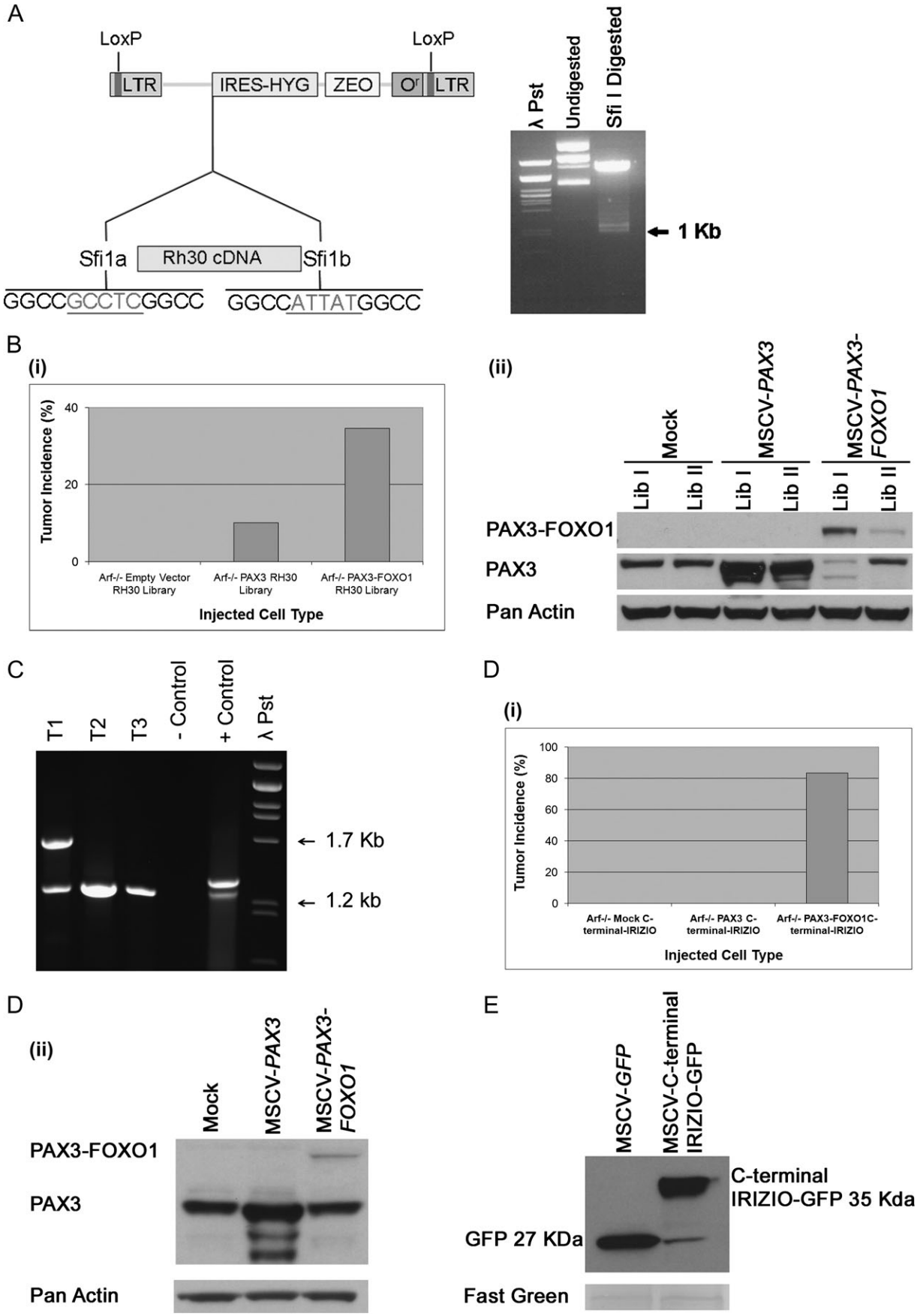

Fig. 1 *In vivo* tumorigenicity of *Arf–/–* myoblasts expressing *PAX3-FOXO1* and a RH30 Marx retroviral expression library. (**A**) Diagram showing the RH30 cDNA library inserted into the modified MarX retroviral vector. Two dissimilar SfiI sites (Sfi1a and Sfi1b) were cloned upstream the IRES-Hygro gene, which

2–4 μg ml^{-1} for RH4; Hygromycin B (Cellgro) was used at a concentration of 200 μg ml^{-1}. Leptomycin B (Sigma) was used at a concentration of 400 nM for 2 h at 37°C.

Histology and immunohistochemistry

Slides of 4–6 μm sections cut from formalin-fixed paraffin-embedded tissues were deparaffinized and rehydrated. For Myogenin and Ki67 stainings, heat-induced epitope retrieval was performed by heating slides in a BioCare Medical Decloaking Chamber at 125°C for 30 s in Target Retrieval buffer (pH 9.0; DAKO, Carpinteria, CA) followed by a 30 min cooldown period. For Desmin, antigen retrieval was performed by heating slides in a BioCare Medical Decloaking Chamber at 125°C for 30 s in citrate buffer (pH 6.0; Invitrogen, Carlsbad, CA) followed by a 30 min cooldown period. Slides were placed in tris buffer saline tween20 buffer (ThermoShandon, Freemont, CA) prior to assay. The following steps were performed on an autostainer at room temperature with tris buffer saline tween20 (ThermoShandon, Freemont, CA) buffer rinses between steps. Endogenous peroxidases were blocked by incubating slides for 5 min with 3% aqueous hydrogen peroxide. For Myogenin, non-specific protein binding was blocked with Background Sniper (30 min; BioCare Medical, Concord, CA). Slides were incubated with mouse anti-human myogenin (clone F5D; DAKO) used at 1:200 for 30 min, then mouse on mouse polymer (BioCare Medical; 30 min) followed by the chromagen 3,3′ diaminobenzidine (DAB, 5 min; ThermoShandon). For Desmin, slides were incubated with mouse anti-Desmin (clone D33; DAKO) used at 1:20 for 30 min, then sequentially with horseradish peroxidase-labeled streptavidin (10 min; ThermoShandon) and the chromagen DAB+ (10 min; DAKO). For Ki67, non-specific protein binding was blocked with Background Sniper (30 min; BioCare Medical). Slides were incubated with anti-human Ki67 (ThermoShandon) used at 1:200 for 30 min, then with Rabbit on Rodent polymer (30 min; BioCare Medical) followed by the chromagen DAB (5 min; ThermoShandon). Slides were counterstained with hematoxylin (ThermoShandon). For PAX3 and hemagglutinin (HA) staining, all assay steps, including deparaffinization, rehydration and any epitope retrieval, were performed on the Bond Max with Bond wash buffer (Leica, Bannockburn, IL) rinses between steps. Heat-induced epitope retrieval was performed by heating slides in ER1 (Leica) for 20 min. The Refine (Leica) detection system was used. Slides were incubated sequentially with hydrogen peroxide (5 min), primary antibody (15 min), post primary (8 min), anti-rabbit or anti-mouse horseradish peroxidase-conjugated polymer (8 min), DAB (10 min) and hematoxylin (5 min). The primary polyclonal anti-PAX3 antibodies (1:500) were purified as described (7). The secondary rabbit anti-goat (Jackson ImmunoResearch, West Grove, PA) was used at 1:600. The mouse anti-HA-Tag (1:1000) was obtained from Cell Signaling Technology (Beverly, MA).

Immunofluorescence

Wild-type and *Arf−/−* primary myoblasts (30×10^5 per well) plated on BD BioCoat collagen type I 4-well culture slides were fixed in 4% paraformaldehyde in phosphate-buffered saline for 15 min on ice. After permeabilization for 10 min in 0.1% Triton in phosphate-buffered saline, cells were blocked in 10% normal goat serum in phosphate-buffered saline and stained with HA antibody (Cell Signaling) and GRP94 antibody (Santa Cruz Biotechnology, Santa Cruz, CA) following the manufacturer's protocol. Bound antibodies were visualized with Alexa 488 goat anti-rabbit (Invitrogen) and Cy3 donkey anti-rat (Jackson Laboratory, Bar Harbor, ME) secondary antibodies. Confocal microscopy was performed on a Nikon TE2000E2 microscope equipped with a Nikon C1Si confocal imaging system using Nikon EZC1 software. Excitation was done with 404, 488 and 561 nm dIode-pumped solid state lasers. Images were acquired with a Nikon ×60 1.45 numerical aperture objective.

Generation of cell/tissue lysates and western blotting

Cells were lysed in Cell Signaling Buffer (Cell Signaling, Beverly, MA) with 1 mM phenylmethylsulfonyl fluoride (1 mM final concentration) or RIPA buffer with Protease (Roche, Indianapolis, IN) and Phosphatase (Sigma) inhibitor cocktails. Available western blots of ARMS primary tumor biopsies were blocked in 5% non-fat milk. Polyclonal anti PAX3 antibodies were diluted 1:1000 in 5% milk; anti-MyoD and anti-myogenin were purchased from Pharmigen (BD Biosciences Pharmingen, San Diego, CA) and used at a concentration of 1.5 μg ml−1 in 5% milk; anti-Myf5 (Santa Cruz Biotechnology) was diluted 1:500 in 5% milk and anti-Myf6 (Aviva, San Diego, CA) 1:1000 in 5% bovine serum albumin (BSA); anti-HA and anti-E2F1 (Cell Signaling) were diluted in 5% BSA following the manufacturer's protocol. Subcellular fractionation was performed using the Qproteome Kit (Qiagen, Alameda, CA). The purity of the cytoplasmic and membrane fractions was determined by western blotting, using glyceraldehyde-3-phosphate dehydrogenase (Chemicon-Millipore, Billerica, MA) and N-Caderin (BD Biosciences, San Jose, CA) antibodies, respectively, both diluted 1:2000 in 5% BSA. The nuclear fraction was stained with Histone H3 antibody (Upstate Biotechnology, Lake Placid, NY) diluted 1:1000 in 5% BSA. Antibodies used for the signaling pathway analysis (supplementary Figure 4 is available at *Carcinogenesis* Online) included anti-total- and phospho-IGFIR, anti-total-Akt and phospho-Akt (Ser 473 and Ser 308), anti-total- and phospho-S6, anti-phospho-Erk1/2 (Thr202/Tyr204) and anti-phospho-p90RSK (Thr359/Ser363), purchased from Cell Signaling Technology and diluted 1:1000 in 5% BSA. Anti-phospho-cJun (Active Motif, Carlsbad, CA) was diluted 1:1000 in 5% BSA. The optical density of IRIZIO (HA) and Pan Actin bands (Figure 3C) was measured using the ImageJ software (http://rsbweb.nih.gov/ij/index.html).

RNA isolation and reverse transcription–PCR

RNA was isolated from myoblasts (2×10^6 cells/10 cm dish) or from ERMS and ARMS cell lines from cultures that were 80% confluent using the MirVANA RNA extraction kit (Applied Biosystems/Ambion, Austin, TX). RNA (1 μg) was used for first strand cDNA synthesis using the SuperScript Double-Stranded cDNA Synthesis Kit (Invitrogen) following the manufacturer's instructions.

For the exon junction analysis, probe/primer sets overlapping splice junctions of *IRIZIO* messenger RNA between exons 6 and 9 were designed using the Primer Express software from Applied Biosystems (Carlsbad, CA). *IRIZIO full-length* splice variant: forward 5′-TGACTGCTGCTACTGTGAGTTCTTC-3′; reverse 5′-GCTTTCTCTCTGCCATTTCCTTT-3′ and probe 5′-ACAATGCGGCAAAAG-3′. *IRIZIOΔ7* variant: forward 5′-GG AAGTTCTGTGACTGCTGCTA-3′; reverse 5′-AGCGGGTGGCGCATT-3′ and probe 5′-TGTGAGTTCTTCGGCC-3′. *IRIZIOΔ7/8* variant: forward 5′-TGACTGCTGCTACTGTGAGTTCTTC-3′; reverse 5′-TGCCAACTGGGCCTTCT-3′ and probe 5′-CAATGC GGAAA-3′. PCRswere performed using the TaqMan Universal PCR Master Mix (Applied Biosystems, Foster City, CA) supplemented with primers, probes and cDNA. Quantification of each splice variant was achieved using a standard curve (expressed in copy number) constructed by amplifying known amounts of target DNA. For *IRIZIOΔ7* and Δ7/*8*, we used the MSCV constructs harboring the cDNA of the two splice variants. For *IRIZIO full-length* including exon 7, we synthesized a specific DNA oligonucleotide corresponding to the exon junction region (exons 6–7): 5′-GGGCTGGGTGAGGAAGAGGATAGCAGCTCTGAGCGAAGCTCCTGCACCTCATCCTCCACCCACCAGAGAGATGGGAAGTTCTGTGACTGCTGCTACTGTGAGTTCTTCGGCCACAATGCGGCAAAAGGAAAGGAAATGGCAGAGAGAAAGCTATGATTCTGATGAGTATGTATACGTGTGTAATCCCAGAGAAGTGAACGCTTGGGAGTGATGAAGGCAGAGTGGAAGCAAAAAGGCTCTC-3′. Expression of target genes was normalized for *GAPDH*. To analyze *IRIZIO* expression after shRNA knockdown, we used a primer/probe set targeting exon 9: forward 5′-GAGCCAAGCTCAAAGGAAGTTC-3′; reverse 5′-GCTTCCCACCTGAGGACACA-3′ and probe 5′-AGGAGCTGCCTGAGC-3′. Standard curve was calculated using serial dilution of MSCV-HA*IRIZIOΔ7* plasmid. *GAPDH* was used as internal control.

allows directional cloning of the cDNAs. The agarose gel on the right shows DNA of the RH30 MarX-cDNA library digested with SfiI. (**B**) (i) Tumor incidence in NOD/SCID mice injected with two independent pools of *Arf−/−* primary myoblasts transduced with empty vector, MSCV-*PAX3* or MSCV-*PAX3-FOXO1* together with the RH30 cDNA library. LibI and LibII indicate the two pools of myoblasts independently transduced with the same library. Tumors generated from MSCV-*PAX3* injected cells developed later those from MSCV-*PAX3-FOXO1* injected cells. (ii) Western blot showing PAX3 and PAX3-FOXO1 expression in *Arf−/−*/MSCV-Puro, *Arf−/−*/MSCV-*PAX3* and *Arf−/−*/MSCV-*PAX3-FOXO1* primary myoblasts also expressing the RH30 MarX library (see supplementary Table I, available at *Carcinogenesis* Online) prior to injection into NOD/SCID mice. (**C**) Agarose gel electrophoresis showing the PCR-amplified products of MarX cDNA proviruses present in the DNA of A*rf−/−*/MSCV-*PAX3-FOXO1/RH30-MarX*-derived tumor cells. T1–T3 represent different tumors from which the cDNAs were amplified. Two specific bands where identified in tumor one: the identity of the upper band will be described elsewhere. The lower band represents the 3′ region of the *FLJ10404/IRIZIO* gene in all three tumors. Genomic DNA extracted from *Arf−/−*/MSCV-*PAX3-FOXO1* cells expressing the RH30 library prior to injection was used as a positive control. Water in the PCR mix was used as a negative control. (**D**) (i) NOD/SCID mice were injected with *Arf−/−* myoblasts expressing empty vector, MSCV-*PAX3* or MSCV-*PAX3-FOXO1* also expressing the Marx-*IRIZIO*-Fragment. Only *Arf−/−*/MSCV-PAX3-FOXO1/MarX-C-terminal-IRIZIO cells produced tumors. (ii) Western blot showing PAX3 and PAX3-FOXO1 expression in MarX-C-terminal-IRIZIO-transduced *Arf−/−/MSCV-PAX3* or A*rf−/−/MSCV-PAX3-FOXO1* primary myoblasts (supplementary Table I is available at *Carcinogenesis* Online). (**E**) Western blot of NIH3T3 cells transiently transfected with expression plasmids encoding GFP or C-terminal-IRIZIO-GFP. Bands were visualized using anti-GFP antibody. Fast green staining of the blot was used as a protein loading control.

Animals

NOD/SCID mice were purchased from the Jackson Laboratory. p*16/Arf−/−* were obtained from Dr David Beach. Mice were maintained at St Jude Children's Research Hospital following the Institutional Animal Care and Use Committee guidelines.

Results

Transformation of primary myoblasts by PAX3-FOXO1 depends upon inactivation of the pRb and p53 pathways

The t(2;13) generating the PAX3-FOXO1 fusion protein is considered the main initiating event in ARMS formation. It has been reported that transformation of muscle progenitors by this oncogene in mice depends on inactivation of both the p53 and pRb tumor suppressor pathways (13). To ascertain that this is also true for cultured low-passage primary mouse myoblasts, we transduced wild-type, *Arf−/−* and p*16/Arf−/−* myoblasts (passage 4) with retroviruses encoding *GFP*, *PAX3* or *PAX3-FOXO1* and tested them for tumor formation by injection (2×10^6 cells per site) into the fore and hind right flanks of –five to six NOD-SCID mice (16). As shown in Table I wild-type or *Arf−/−* myoblasts transduced with these retroviruses did not form tumors during the 6 months observation period, whereas p*16/Arf−/−/PAX3-FOXO1* myoblasts produced five tumors within 4–6 weeks. In comparison, p*16/Arf−/−/GFP* myoblasts produced one tumor after 4 months and p*16/Arf−/−/PAX3* myoblasts produced four tumors after 2–6 months, appearing considerable later than p*16/Arf−/−/PAX3-FOXO1* tumors. This experiment showed that transformation of myoblasts by PAX3-FOXO1 is dependent on combined compromised p53/pRb pathways.

C-terminal IRIZIO cooperates with PAX3-FOXO1 to transform Arf−/− primary mouse myoblasts

Based on these results, we set out to identify novel genes that might cooperate with *PAX3-FOXO1* in the transformation of *Arf−/−* mouse primary myoblasts. We generated a cDNA library from the RH30 ARMS cell line (12) in a modified Marx retroviral vector (17) (Figure 1A). Two independent pools of *Arf−/−* myoblasts stably expressing MSCV-SV40-Puro, MSCV-*PAX3*-SV40-Puro or MSCV-*PAX3-FOXO1*-SV40-Puro were transduced with the RH30 retroviral cDNA library (LibI and LibII, Figure 1B, panel ii) and the resulting hygromycin resistant cell pools were subcutaneously injected into the right fore- and hind flanks of NOD/SCID mice (supplementary Table I, upper panel, is available at *Carcinogenesis* Online). Tumor formation was monitored for up to 5 months post injection. Within this observation period, 7 of 13 mice injected with both *Arf−/−/PAX3-FOXO1*/MarX-RH30 cell pools developed tumors within 4–8 weeks, generating a total of nine tumors resulting in a tumor incidence of 34.6% (Figure 1B, panel i). Two mice injected with *Arf−/−/PAX3*/MarX-RH30 cells also developed tumors but only after 10 and 14 weeks post injection, respectively, resulting in a tumor incidence of 10%. *Arf−/−/MSCV-Puro*/MarX-RH30 injected mice did not develop tumors. The cooperating cDNAs were recovered from the genomic DNA of the PAX3-FOXO1 tumors by PCR (Figure 1C), subcloned and sequenced. Three of six analyzed tumors contained a cDNA encoding part of the hypothetical protein FLJ10404, which we dubbed IRIZIO. In all cases, an identical partial cDNA sequence was found, all starting with a GTG codon, which when used as a start codon would result in a C-terminal IRIZIO open reading frame (ORF) of 227 amino acids. An in-frame ATG codon was also present downstream of the GTG, potentially encoding a further truncated C-terminal IRIZIO peptide of 49 amino acids. We next determined which portion of C-terminal IRIZIO was encoded by the cDNA fragment by fusing it in-frame to the 5′ end of the GFP ORF in the MSCV retroviral vector. Lysates of NIH3T3 cells transiently transfected with this IRIZIO-GFP construct were immunoblotted using GFP antibodies (Figure 1E), showing a fusion protein of ∼34 kDa. Thus, the IRIZIO peptide measured a mere 7 kDa given that the size of GFP protein is 27 kDa, indicating that translation starts at the first in-frame ATG, which matches the consensus Kozak translation initiation sequence (12).

To verify cooperation between the isolated cDNA and *PAX3-FOXO1*, we reinserted the partial *IRIZIO* cDNA into the MarX vector and transduced a second pool of *Arf−/−* myoblasts expressing MSCV-SV40-Puro, MSCV-*PAX3*-SV40-Puro or MSCV-*PAX3-FOXO1*-SV40-Puro. Only NOD/SCID mice (Figure 1D; supplementary Table I is available at *Carcinogenesis* Online, lower panel) injected with *Arf−/−/PAX3-FOXO1*/MarX-*IRIZIO* myoblasts developed tumors 3–4 weeks after the injection. This confirmed that the 3′ *IRIZIO* retrovirus cooperated with PAX3-FOXO1 in the neoplastic transformation of primary Arf−/− myoblasts.

Arf−/−/PAX3-FOXO1/C-terminal-IRIZIO tumors resemble ARMS tumors at the morphological and molecular level

To determine the morphology and molecular characteristics of the *Arf−/−/PAX3-FOXO1*/C-terminal-IRIZIO tumors in NOD/SCID mice, we prepared paraffin sections and isolated hygromycin and puromycin resistant cell lines from these tumors. Tumors were diagnosed by histopathology and immunohistochemistry to be the solid variant of ARMS (Figure 2A). The tumors were highly infiltrative into the surrounding muscle, and residual host muscle fibers were scattered within the mass, predominately along the margins. Although there were no prominent fibrous septae as are typical for ARMS, the cells were arranged in ill-defined aggregates with central loss of cellular cohesiveness. The skeletal muscle origin of the tumors was confirmed by scattered diffuse positive staining for myogenin and multifocal areas of positive desmin expression. Affinity-purified PAX3 antibody showed expression of endogenous PAX3 and exogenous PAX3-FOXO1. Sections were also stained with Ki67 antibody, which stains proliferating cells in all phases of the cell cycle (supplementary Figure 1 is available at *Carcinogenesis* Online), confirming the neoplastic nature of *Arf−/−/PAX3-FOXO1*/C-terminal-*IRIZIO* tumors. To further investigate whether the *Arf−/−/PAX3-FOXO1*/C-terminal-*IRIZIO* fragment tumors resembled primary ARMS at the molecular level, we performed western blot analysis using cell lysates from *Arf−/−* injected myoblasts, tumor cells and primary ARMS tumor biopsies using antibodies detecting muscle cell-specific differentiation markers (Figure 2B). Except for Myf5, the murine *IRIZIO*

Table I. NOD/SCID mice were subcutaneously injected in the fore and hind right flanks with WT, *Arf−/−* or p*16/Arf−/−* primary mouse myoblasts transduced with MSCV-GFP, MSCV-*PAX3*-GFP or MSCV-*PAX3-FOXO1*-GFP retrovirus

Primary myoblast	Construct	Number of injected mice	Number of injections per mouse	Mice with tumors	Total number of tumors	Time of tumor formation
WT	MSCV-GFP	2	2	0	0	—
WT	MSCV-*PAX3*	2	2	0	0	—
WT	MSCV-*PAX3-FOXO1*	2	2	0	0	—
Arf−/−	MSCV-GFP	2	2	0	0	—
Arf−/−	MSCV-*PAX3*	2	2	0	0	—
Arf−/−	MSCV-*PAX3-FOXO1*	4	2	0	0	—
Arf−/−/p16−/−	MSCV-GFP	5	2	1	1	4 months
Arf−/−/p16−/−	MSCV-*PAX3*	5	2	4	4	2–6 months
Arf−/−/p16−/−	MSCV-*PAX3-FOXO1*	6	2	4	5	4–6 weeks

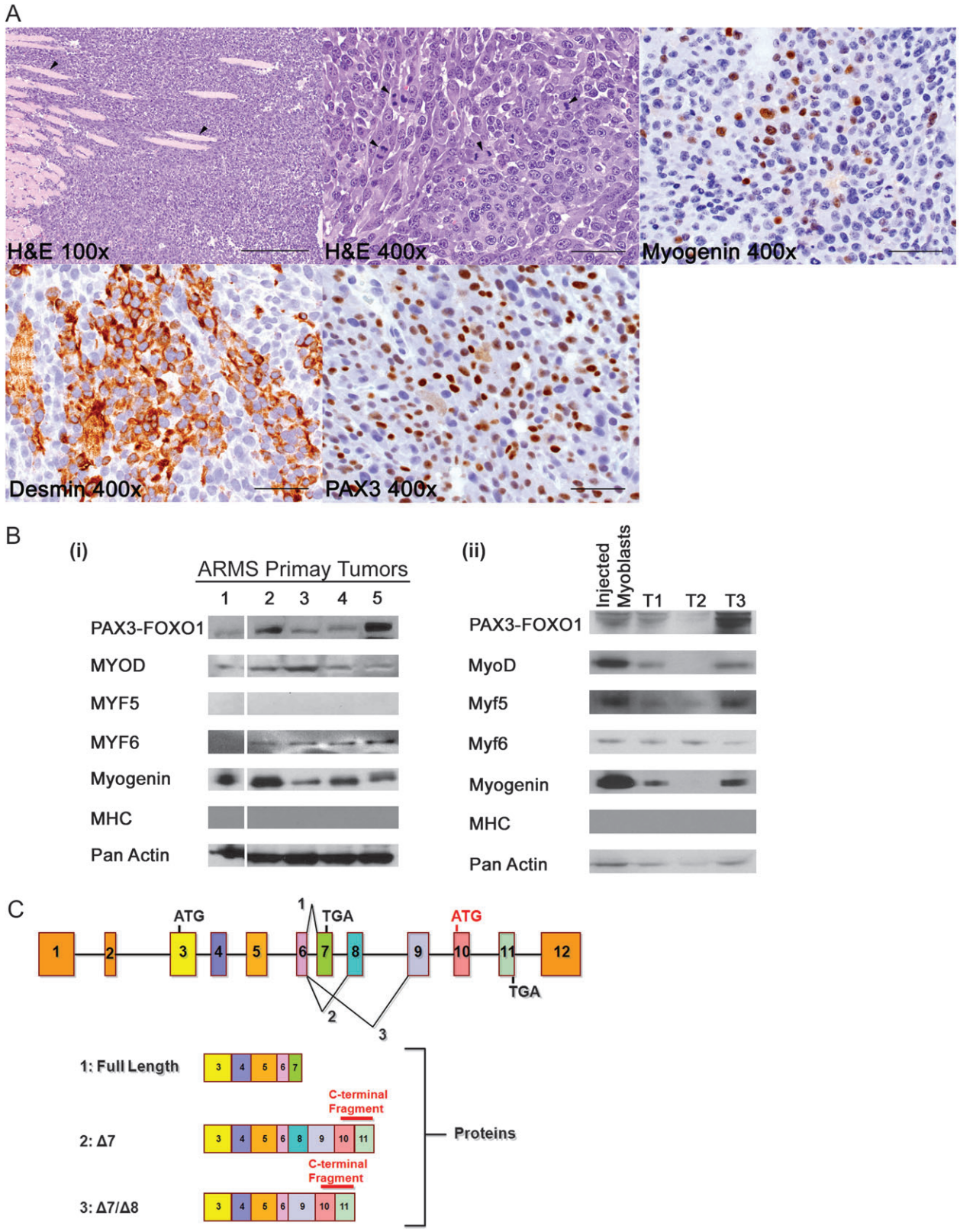

Fig. 2 C-terminal-IRIZIO-derived tumors express similar molecular markers as ARMS primary tumors. (**A**) Tumor sections derived from mice injected with *Arf−/−/PAX3-FOXO1/C-terminal-IRIZIO* myoblasts were stained with hematoxylin and eosin, with Myogenin, Desmin or PAX3 antibodies. Scale bars in images: ×100 magnification scale bar, 250 μm; ×400 magnification scale bar, 50 μm. The arrowheads in the ×100 hematoxylin and eosin image indicate muscle fibers, which are being separated by the tumor. In the ×400, they indicate mitotic figures. (**B**) Western blot showing expression of the muscle cell-specific markers MyoD, Myf5, Myf6 and Myogenin in five primary ARMS tumors (i) and *Arf−/−/PAX3-FOXO1/C-terminal-IRIZIO* tumors (ii). Pre-injection *Arf−/−/PAX3-FOXO1/C-terminal-IRIZIO* cells were used as control. (**C**) The *IRIZIO* gene is located on chromosome 5 and is composed of 12 exons. The splice variant 1 (full length) contains exon 7 and generates a truncated protein due to the presence of a stop codon in the ORF. The variants Δ7 and Δ7/8 encode larger proteins. The portion of the protein encoded by the C-terminal IRIZIO cDNA is indicated by the red line above the Δ7 and Δ7/8 proteins.

fragment-derived tumors and the human ARMS tumors expressed similar differentiation markers (Figure 2B). Therefore, tumors generated by cells expressing the *Arf−/−/PAX3-FOXO1*/C-terminal-*IRIZIO* fragment showed both morphological and molecular similarity with primary ARMS.

IRIZIO encodes at least three differentially spliced messenger RNAs but only two transform *PAX3-FOXO1* expressing *Arf−/−* myoblasts.

To establish that also full-length IRIZIO transformed *Arf−/−*/PAX3-FOXO1 myoblasts, we queried the Ensembl database and found that three alternatively spliced transcripts are known for human IRIZIO (Figure 2C). Although more splice variants are listed for the human gene, only one is listed for the mouse. Because of this, we focused our attention to the splice form that is present in both mouse and human. IRIZIO shows high sequence conservancy among mammals, especially at the 3′ end of the ORF. Human *IRIZIO* is located on chromosome 5 and is composed of 12 exons with an ORF starting in exon 3. Sequence alignment between human and mouse full-length transcripts showed an overall homology of 80%. Alternative splicing involves exons 7 and 8 (Figure 2C). Exon 7 contains a stop codon in the ORF, resulting in a truncated protein lacking the carboxy-terminal region. Splicing out exon 7 (*Δ7*) or exons 7 and 8 (*Δ7/8*) would generate larger proteins that both include the C-terminal IRIZIO peptide described above. DNA and protein sequences of IRIZIO *Δ7* and *Δ7/8* are reported in supplementary Figure 2 (available at *Carcinogenesis* Online). The existence of the *Δ7* and *Δ7/8* splice variants was confirmed by semi-quantitative reverse transcription–PCR using RNA from ARMS and ERMS cell lines, several human tissues and primers specific for exons 5 and 9. The identity of each cDNA was verified by sequence analysis (data not shown). The reverse transcription–PCR did not detect the splice variant including exon 7. Therefore, we only cloned cDNAs for *the Δ7* and *Δ7/8* splice variants into the MSCV-I-GFP retroviral vector. Because there are no suitable commercial antibodies available for IRIZIO, an N-terminal HA tag was added to each construct. We repeated the *in vivo* transformation experiments by expressing the HA-*Δ7* and HA-*Δ7/8 IRIZIO* variants in *Arf−/−/*vector, Arf−/−/PAX3 and *Arf−/−/PAX3-FOXO1* myoblasts. Lysates obtained from cells prior to injection were immunoblotted with PAX3 and HA antibodies to confirm expression of HA-PAX3-FOXO1 and IRIZIO (Figure 3B). All mice injected with IRIZIOΔ7 expressing myoblasts developed a subcutaneous tumor within 8 weeks postinjection resulting in a higher tumor incidence (50%) than in mice injected with IRIZIOΔ7/8 expressing cells, which formed two independent tumors in one animal, 13 weeks postinjection (tumor incidence of 20%; Table II and Figure 3A). Sections from paraffin-embedded *PAX3-FOXO1/HA*-IRIZIO*Δ7* tumors were immunostained with HA, PAX3, Myogenin, Desmin and Ki67 antibodies, confirming expression of all these proteins (Figure 3D; supplementary Figure 1 is available at *Carcinogenesis* Online). Histologically, the PAX3-FOXO1/HA-IRIZIO*Δ7* tumors showed the classic pattern for ARMS, including distinct fibrous septae and central loss of cellular cohesiveness. Many cells had positive staining for myogenin and nearly all cells stained positively for Desmin. Lysates of cultured cells isolated from the excised tumors were immunoblotted for the expression of PAX3, HA–IRIZIOΔ7 and muscle-specific differentiation markers, showing an expression pattern similar to that of primary ARMS tumors (Figures 2B and 3C). Analysis of tumors derived from *Arf−/−/PAX3-FOXO1/HA*-IRIZIO*Δ7/8* myoblasts showed identical results (data not shown) suggesting that the IRIZIO*Δ7/8* splice variant operates similar to IRIZIO*Δ7*, albeit with reduced efficiency. To determine if the C-terminal region of IRIZIO is necessary for transformation, we also tested the *in vivo* tumorigenicity of two HA-IRIZIO*Δ7* deletion mutants also lacking part of exon 10 and the entire exon 11 (HA-*IRIZIOΔ7/Δ10-11*) or exons 9–11 (HA-*IRIZIOΔ7/Δ*9-11). We compared tumor formation in mice injected with *Arf−/−/PAX3-FOXO1* myoblasts expressing vector, *HA-IRIZIOΔ7*, HA-*IRIZIOΔ7/Δ10-11* or HA-*IRIZIOΔ7/Δ*9-11 over a period of 5 months (Table II). All mice injected with myoblasts expressing the HA-IRIZIO*Δ7* splice variant readily developed tumors during this time period (within 4–8 weeks, tumor incidence 80%) but also two mice injected with HA-*IRIZIOΔ7/Δ10-11* developed a tumor (within 8–9 weeks, tumor incidence 20%), whereas HA-*IRIZIOΔ7/Δ*9-11 injected mice remained healthy (Figure 3E). Because the level of expression of all IRIZIO constructs was similar (Figure 3B and E, panel ii), this suggested that *IRIZIO Δ7* transformed *Arf−/−/PAX3-FOXO1* myoblasts more efficiently than splice variant HA-*IRIZIOΔ7/8* or the deletion mutant HA-*IRIZIOΔ7/Δ10-11*. Moreover, the C-terminal region encoded by exons 9–11 of *IRIZIO Δ7* is essential for transformation.

The IRIZIOΔ7 splice variant is overexpressed in ERMS and ARMS cell lines

Alternative splicing events affect the functional diversity of a large number of genes (18). Alternative splicing is crucial for normal development and physiology of numerous tissues and organs and deregulation has been associated with human disease (19, 20). To determine the abundance of each *IRIZIO* splice variant in ARMS cell lines, we performed a quantitative exon junction real-time PCR using specific primers/probe sets in the region between exons 6 and 9. We used cDNAs from several ERMS and ARMS cell lines and cDNA from proliferating and differentiating primary human myoblasts was used as a control (Figure 4A). This showed that the full-length 12 exon variant is least abundant in both ERMS and ARMS cell lines. Conversely, the *Δ7* variant appeared to be upregulated in both ERMS and ARMS cell lines compared with the primary human myoblasts at any stage of differentiation, whereas there was no significant change in the expression level of *Δ7/8 RNA*. This is in agreement with our observation that the *Δ7* splice variant cooperated with *PAX3-FOXO1* in the transformation of Arf−/− myoblasts. However, upregulation of *IRIZIOΔ7* also

Table II. NOD/SCID mice were subcutaneously injected in the fore and hind flanks (right side) with *Arf-/-/*MSCV-Puro, *Arf-/-/*MSCV-*PAX3-Puro* or Arf−/−/MSCV-*PAX3-FOXO1-Puro* primary myoblasts also transduced with MSCV-HAIRIZIO*Δ7*–GFP or MSCV-HAIRIZIO*Δ7/8*–GFP retrovirus

Primary myoblast background	Cooperating genes	Construct	Number of injected mice	Number of injections per mouse	Mice with tumors	Total number of tumors	Time of tumor formation
Arf−/−	MSCV-HA *IRIZIOΔ7*-GFP	MSCV-SV40-Puro	5	2	0	0	—
Arf−/−	MSCV-HA *IRIZIOΔ7*-GFP	MSCV-*PAX3*-SV40-Puro	5	2	0	0	—
Arf−/−	MSCV-HA *IRIZIOΔ7*-GFP	MSCV-*PAX3-FOXO1*-SV40-Puro	5	2	5	5	8–10 weeks
Arf−/−	MSCV-HA *IRIZIOΔ7/8*-GFP	MSCV-SV40-Puro	5	2	0	0	—
Arf−/−	MSCV-HA *IRIZIOΔ7/8*-GFP	MSCV-*PAX3*-SV40-Puro	5	2	0	0	—
Arf−/−	MSCV-HA *IRIZIOΔ7/8*-GFP	MSCV-*PAX3-FOXO1*-SV40-Puro	5	2	1	2	13 weeks
Arf−/−	GFP	MSCV-*PAX3-FOXO1*-SV40-Puro	5	2	0	0	
Arf−/−	MSCV-HA *IRIZIOΔ7*-GFP	MSCV-*PAX3-FOXO1*-SV40-Puro	5	2	5	6	5–8 weeks
Arf−/−	MSCV-HA *IRIZIOΔ7/Δ10-11*-GFP	MSCV-*PAX3-FOXO1*-SV40-Puro	5	2	2	2	7–12 weeks
Arf−/−	MSCV-HA *IRIZIOΔ7/Δ9-11*-GFP	MSCV-*PAX3-FOXO1*-SV40-Puro	5	2	0	0	—

The relative tumorigenicity of the *IRIZIO* deletion mutants was evaluated by injecting NOD/SCID mice with Arf−/−/*PAX3-FOXO1* myoblasts expressing HA-*IRIZIOΔ7/Δ10-11* or HA-*IRIZIOΔ7/Δ9-11*. Cells expressing HA-*IRIZIOΔ7* were used as a positive control.

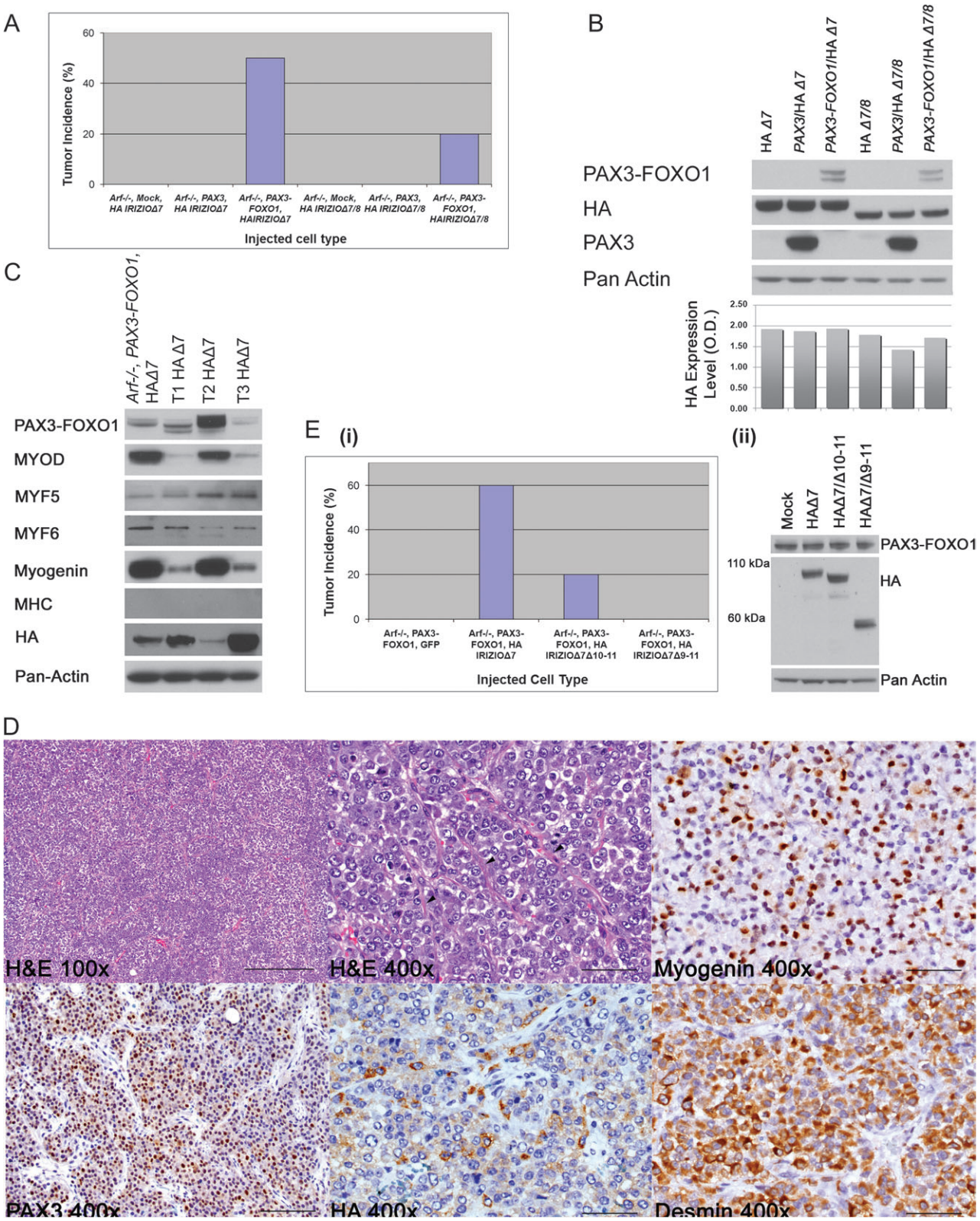

Fig. 3 *IRIZIO Δ7 and Δ7/8* splice variants cooperate with *PAX3-FOXO1A* to transform Arf−/− primary myoblasts. (**A**) Tumor incidence in NOD/SCID mice injected with Arf−/− primary myoblasts transduced with empty vector, MSCV-*PAX3* or MSCV-*PAX3-FOXO1* and also transduced with MSCV-HA-*IRIZIOΔ7*–GFP or MSCV-HA-*IRIZIOΔ7/8*–GFP retrovirus. Tumor formation in HA-*IRIZIOΔ7* injected mice occurred within 8–10 weeks post injection, whereas mice injected with HA-*IRIZIOΔ7/8* developed tumors 13 weeks after injection (Table II). Results were obtained from two independent experiments. (**B**) Western blots of Arf−/− myoblast expressing MSCV-HA-*IRIZIOΔ7*–GFP or MSCV-*HA-IRIZIOΔ7/8*–GFP injected into NOD/SCID mice (Table II). PAX3 and HA antibodies were used for the detection of PAX3 or PAX3-FOXO1 and IRIZIO splice variants, respectively. Pan Actin antibody was used as a control for equal protein loading. The histogram underneath the blot shows the relative intensity of IRIZIOΔ7 and Δ7/8 bands as calculated by normalizing the optical density (O.D.) of the HA-IRIZIO bands with that of the Pan-Actin bands. (**C**) Western blot analysis of *IRIZIOΔ7*–GFP tumor cells isolated from tumors listed in Table II using HA, PAX3, MyoD, Myf5, Myf6 or Myogenin antibodies. Pan-actin staining was used as a loading control. But for Myf5, the expression pattern of myogenic markers in

occurs in ERMS tumor cell lines thereby excluding exclusive cooperation with *PAX3-FOXO1*. Thus, *IRIZIOΔ7* overexpression might be an additional event contributing to transformation of myogenic progenitor cells, suggesting that overexpression of the Δ7 splice variant might play a causative role in human rhabdomyosarcomagenesis.

We next addressed if knockdown of *IRIZIO* in *Arf−/−/PAX3-FOXO1/IRIZIOΔ7* cells isolated from a tumor in NOD/SCID mice would suppress their *in vivo* tumorigenicity. After subcutaneous injection into mice, cells transduced with IRIZIO shRNA retrovirus or control non-targeting shRNA virus, showing 80% and no knockdown of IRIZIO protein, respectively (supplementary Figure 3A is available at *Carcinogenesis* Online), developed tumors equally efficiently (supplementary Figure 3B is available at *Carcinogenesis* Online). A repeat experiment with the ARMS RH4 cell line, comparing non-targeting shRNA cells with cells that showed a 75% knockdown of IRIZIO RNA, resulted in equally efficient tumor formation (data not shown) in NOD-SCID mice. This suggested that IRIZIO expression is important during tumor formation, but once established IRIZIO expression is dispensable for maintaining the transformed state.

Subcellular localization of IRIZIO variants

To determine the subcellular localization of HA-IRIZIOΔ7 and HA-IRIZIOΔ7/8, we performed immunostaining with an HA antibody of primary *Arf−/−* myoblasts expressing these proteins. Confocal microscopy showed that both splice variants localized in the cytoplasm with increased fluorescence signal in the perinuclear region. To further define this staining pattern, we performed a co-immunostaining with an antibody specific for the endoplasmatic reticulum protein GRP94 (Figure 4B, panels i and ii). This showed partial colocalization with the IRIZIOΔ7 and IRIZIOΔ7/8 signals. Because the C-terminal region of IRIZIO stimulates PAX3-FOXO1's transforming activity, we repeated the experiment with *Arf−/−* myoblasts expressing the HA-*IRIZIOΔ7/Δ10-11* or HA-*IRIZIOΔ7/Δ9-11* mutants to determine whether this region affected protein localization. HA-IRIZIOΔ7/Δ10-11 showed a staining pattern identical to that of the other splice variants (Figure 4B, panel iii) suggesting that the region encoded by exons 10 and 11 does not affect protein localization. However, the mutant lacking the sequences encoded by exon 9 to exon 11 showed a mostly nuclear staining. Hence, the sequences encoded by exon 9 maintain the protein in the cytoplasm, indicating that IRIZIO probably shuttles between the cytoplasm and nucleus with the equilibrium of transport strongly toward the cytoplasmic side (Figure 4B, panel iv). To exclude that PAX3-FOXO1 protein had any effect on IRIZIO localization, we repeated the same immunostaining experiments with *Arf−/−/PAX3-FOXO1* myoblasts, which produced identical results (data not shown). Sequence analysis of the IRIZIO C-terminal region identified a putative bipartite NLS (21) –KRARHKLKKK– at the 3′ end of exon 8 and a putative leucine-rich nuclear export signal (NES) (22) –LDLSPLTL– in exon 9 (Supplementary Figure 2 is available at *Carcinogenesis* Online). To test if IRIZIO indeed shuttles, we transduced primary *Arf−/−* myoblasts with MSCV-HA-*IRIZIOΔ7*-GFP, MSCV-HA-*IRIZIOΔ7/8*-GFP, MSCV-HA-*IRIZIOΔ7/Δ9-11*-GFP or MSCV-HA-*IRIZIOΔ7/Δ10-11*-GFP retrovirus and plated GFP^+-sorted cells on collagen-coated glass slides and treated the cells for 2 h with vehicle or Leptomycin B, which blocks CRM1-mediated nuclear export. Immunostaining with HA antibody (supplementary Figure 4 is available at *Carcinogenesis* Online) showed that HA-IRIZIOΔ7, HA-IRIZIOΔ7/8 and HA-IRIZIOΔ7/Δ10-11 localized in the nucleus of Leptomycin B-treated cells, whereas in vehicle-treated myoblasts, these proteins resided in the cytoplasm. No difference in localization was observed in cells expressing the HA-IRIZIOΔ7/Δ9-11 mutant lacking the NES sequence. Our results therefore confirmed the nuclear-cytoplasmic shuttling nature of IRIZIO. We also analyzed IRIZIO localization by western blotting using subcellular fractions of *Arf−/−* myoblasts overexpressing HA-*IRIZIOΔ7*, HA-*IRIZIO*Δ7/8, HA-*IRIZIOΔ7/Δ9-11* or HA-*IRIZIOΔ7/Δ10-11* (Figure 4C). This confirmed the cytoplasmic localization of the first three proteins but paradoxically the *IRIZIOΔ7/Δ*9-11 also appeared in the cytoplasmic fraction. We believe this to be an artifact of the subcellular fractionation procedure given that immunostaining showed nuclear localization. Together, these results indicated that IRIZIOΔ7 and IRIZIOΔ7/8 mainly localize in the cytoplasm of primary mouse myoblasts and they partially colocalized with the endoplasmic reticulum.

Discussion

Cancer is a multistep process involving several cooperating mutations in oncogenes and tumor suppressor genes (23). In this paper, we utilized an *in vivo* genetic screen to identify novel cooperating partners for PAX3-FOXO1, the pathognomonic sign of ARMS. The screen was based on the observation that PAX3-FOXO1 transforms mouse primary myoblasts that harbor a compromised p53 and pRb pathway (11, 13). We transduced primary mouse myoblasts with a compromised p53 pathway (*Arf−/−*) stably expressing *PAX3-FOXO1* with a retroviral cDNA expression library generated from the fully transformed ARMS cell line RH30. We expected that cooperating cDNAs would interfere directly or indirectly with the pRb pathway. After injection of these cells into NOD-SCID mice, three independent tumors carried a cDNA representing the 3′ half of exon 9 and exons 10 and 11 of *IRIZIO*, encoding a 49 amino acid C-terminal polypeptide. Despiting using a full-length cDNA cloning strategy, the IRIZIO clone isolated from the library was a partial cDNA because full-length IRIZIO cDNA does not contain Sfi1 restriction sites. A multispecies alignment of the *IRIZIO* transcript (Ensembl gene ID: ENSG00000146067) revealed that the coding exons are highly conserved among mammals. We identified three messenger RNA species generated by differential splicing for human *IRIZIO*; the longest coding isoform (full length) contained a stop codon in exon 7 resulting in a truncated protein lacking the 49 amino acid C-terminal region. Because of this and the *Δ7* transcript listed for the mouse in the Ensembl database, we focused our attention on the other two splice variants Δ7 and Δ7/8, which produced proteins that contain the 49 amino acid C-terminus. In silico analysis of the IRIZIO Δ7 and Δ7/8 secondary structures using the conserved domain database on the National Center for Biotechnology Information website revealed no obvious homology to any known domain present in the database. IRIZIO belongs to the FAM193 gene family together with the Cr8Orf gene. The official name for those genes is 'family with sequence similarity 193, member B (FAM193B) or member A (FAM193A)', respectively. Protein sequence alignment between IRIZIOΔ7 and FAM193A using the National Center for Biotechnology Information Basic Local Alignment Search Tool revealed an overall homology of 53%. Interestingly, the highest similarity is in the last 76 amino acids (89% homology) of both proteins, which includes the library-isolated C-terminal IRIZIOΔ7 sequence. This sequence was also analyzed using the SWISS-MODEL and InterProScan databases (24, 25). This secondary structure analysis showed that IRIZIO is composed of random coil regions (77.4%), alpha-helices (19.5%) and extended beta sheets (3.1%), suggesting that IRIZIO is largely an unfolded polypeptide lacking any fixed three-dimensional structure.

Mice injected with *Arf−/−IRIZIOΔ7/PAX3-FOXO1* myoblasts produced tumors in 50% of the injection sites after 8 weeks, whereas in mice injected with *Arf−/−/IRIZIO*Δ7/8*/PAX3-FOXO1* myoblasts,

IRIZIOΔ7 tumors was similar to that in primary ARMS tumors (Figure 2). (**D**) Hematoxylin and eosin, Myogenin, Desmin, PAX3 or HA staining of tumor sections derived from mice injected with *Arf−/−/PAX3-FOXO1*/HA-*IRIZIOΔ7*–GFP myoblasts. Scale bars in images: ×100 magnification scale bar, 250 μm; ×400 magnification scale bar, 50 μm. The arrowheads in ×400 hematoxylin and eosin image indicate the fibrous septae. (**E**) (i) NOD/SCID mice, subcutaneously injected with 2×10^6 *PAX3-FOXO1/Arf−/−* myoblasts expressing HA-*IRIZIOΔ7* or the HA-*IRIZIOΔ7/Δ10-11* or HA-*IRIZIOΔ7/Δ9-11* mutants, developed tumors at 5–8 weeks, 7–12 weeks or no tumors within the 6 months observation period, respectively (Table II). (ii) Western blot showing expression of HA-IRIZIOΔ7, HA-IRIZIOΔ7/Δ10-11 or HA-IRIZIOΔ7/Δ9-11 in *Arf−/−*/PAX3-FOXO1 cells using an HA antibody prior to injection into NOD/SCID mice. Pan actin staining was used as a loading control.

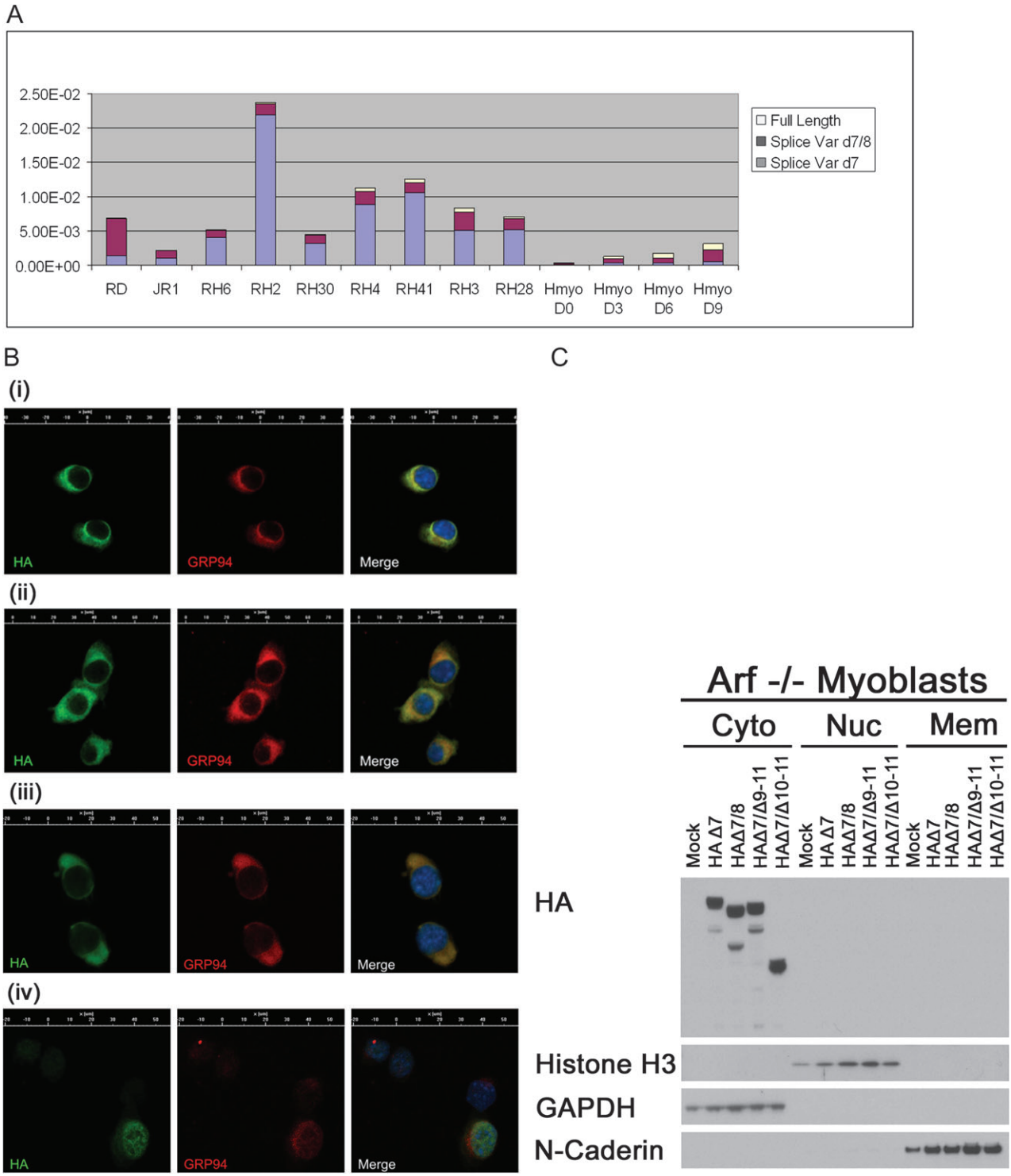

Fig. 4 I*RIZIO Δ7* is overexpressed in ERMS and ARMS cell lines. (**A**) Graph showing the expression pattern of *IRIZIO* splice variants in ERMS (RD, JR1, RH6 and RH2) and ARMS (RH30, RH4, RH41, RH3 and RH28) cell lines determined by quantitative real-time reverse transcription–PCR analysis. Expression level of the differentially spliced *IRIZIO* variants was obtained using primer/probe sets specific for the exon junction region of each variant, between exon 6 and exon 9. Proliferating (D 0) and differentiating (D3–D9) primary human myoblasts were used as a control for wt *IRIZIO* expression. (**B**) Immunohistochemistry of *Arf−/−* primary myoblasts expressing HA-*IRIZIOΔ7*-GFP (i), HA-*IRIZIOΔ7/8*-GFP (ii), HA-*IRIZIOΔ7/Δ10-11*-GFP (iii) HA-*IRIZIOΔ7/Δ9-11* (iv). Proliferating myoblasts grown on collagen-coated slides were stained with antibodies against the ER protein GRP94 and HA. Confocal images were taken using a Nikon (TE2000E2) microscope at ×600 magnification. (**C**) Western blot analysis performed on subcellular fractions of *Arf−/−* primary myoblasts expressing HA-*IRIZIOΔ7*-GFP, HA-*IRIZIOΔ7/8*-GFP, HA-*IRIZIOΔ7/Δ10-11*-GFP or HA-*IRIZIOΔ7/Δ9-11-GFP*. To determine the purity of each fraction, the blot was probed using antibodies for glyceraldehyde-3-phosphate dehydrogenase (Cytosol), Histone H3 (Nucleus) and N-Cadherin (Membranes). IRIZIO proteins were visualized using HA antibodies.

only 20% of the injection sites produced tumors after 12 weeks. This suggested that the region encoded by exon 8 affected *IRIZIO's* transforming activity. It is noteworthy that we identified a putative bipartite NLS in exon 8 and a putative leucine-rich NES in exon 9. The localization experiments using the combination of the IRIZIO*Δ*7/*Δ*9-11 mutant and the Leptomycin B nuclear export inhibitor strongly

suggest that IRIZIOΔ7 is shuttling through the nucleus and that the potentially resulting posttranslational modifications of the protein may be important for its transforming activity in combination with PAX3-FOXO1. Additional experiment will have to show the functionality of the putative NLS and NES.

Tumor formation by *Arf−/−/IRIZIOΔ7/PAX3-FOXO1* myoblasts was delayed compared with tumors generated by *Arf−/−/PAX3-FOXO1* myoblasts expressing the *IRIZIO* C-terminal fragment. Also, tumors generated with IRIZIOΔ7 seemed more differentiated than those with the C-terminal fragment, as evidenced by the higher level of myogenin staining and the diffuse expression of Desmin. Because this fragment measures 49 amino acids, it is reasonable to speculate that it will bind to another protein(s), thereby altering the activity of this target rather than having a direct enzymatic or structural function of its own. Currently, we have not yet identified potential interaction partners of the IRIZIO peptide. We also determined if presence of the C-terminal peptide was essential for the transforming activity of IRIZIOΔ7 and found that the protein missing the peptide (*IRIZIOΔ10-11*) displayed reduced transforming activity. This suggests that the peptide is important but not essential for IRIZIOΔ7's transforming activity, whereas a mutant missing a larger part of the C-terminus (*IRIZIOΔ9-11*) locating to the nucleus had no transforming activity. Thus, although the 49 amino acid peptide alone is sufficient to cooperate with PAX3-FOXO1 in transformation, the entire domain mediating cooperation may extend further N-terminal although we have not mapped the boundary of this extension.

An exon junction real time reverse transcription–PCR showed that compared with primary human myoblasts the IRIZIO*Δ7* transcript is overexpressed in ERMS and ARMS cell lines, whereas the full-length variant appeared to be the least abundant in all samples. Our IRIZIO knockdown experiments suggest that the protein plays a role in tumor formation but not in tumor maintenance. Both in mouse Arf−/−/PAX3-FOXO1/IRIZIO*Δ7* tumor cells and the ARMS cell line RH4, knockdown of IRIZIO*Δ7* did not affect the *in vivo* tumorigenicity. To understand whether IRIZIO*Δ7* or IRIZIO*Δ7/Δ8* expression affects signaling pathways that might feed into the Rb pathway, we checked the phosphorylation status of Akt, Erk1/2, p90, cJun and S6 in Arf−/− myoblasts expressing PAX3-FOXO1 in combination with GFP, IRIZIO*Δ7* or IRIZIO*Δ7/Δ8*, but no obvious differences were noted (supplementary Figure 5 is available at *Carcinogenesis* Online). We also looked for changes in the cellular localization of E2F1, but again, E2F1 remained in the cytoplasm of the different myoblast cell lines (supplementary Figure 6 is available at *Carcinogenesis* Online).

Despite the lack of an obvious link with the pRb pathway, our *IRIZIOΔ7* data are consistent with the observation that overexpression of IRIZIO messenger RNA is associated with recurrent lung tumor formation in a specific subgroup of patients (26), confirming that IRIZIO can function as an oncogene in other tumors also. This is in agreement with our data that IRIZIO RNA is upregulated both in ARMS and ERMS cell lines excluding a unique cooperation between PAX3-FOXO1 and IRIZIO. Additional studies are required to determine which IRIZIO splice variant is overexpressed in those lung cancer patients to better understand the function of this novel oncogene in human tumorigenesis.

Supplementary material

Supplementary Figures 1–6 and Table I can be found at http://carcin.oxfordjournals.org/

Funding

Van Vleet Foundation of Memphis; Cancer Center (Core, CA021765); American Lebanese Associated Charities of St Jude Children's Research Hospital.

Acknowledgements

We thank Dr David Beach for providing the MarX expression vector, Amy Marshall for help with real-time PCR analysis, Frank Harwood, Ramon Klein Geltink, Ayten Kandilci and Sabrina Terranova for help and reagents. We thank Margaret Hall for secretarial work, Simon Moshiach for help with confocal microscopy, Tanya Kranenburg and Julie McAuley for reading the manuscript and the St Jude fluorescence activated cell sorting Core facility for cell sorting.

Conflict of Interest Statement: None declared.

References

1. Merlino,G. *et al*. (1999) Rhabdomyosarcoma—working out the pathways. *Oncogene*, **18**, 5340–5348.
2. Barr,F.G. (2001) Gene fusions involving PAX and FOX family members in alveolar rhabdomyosarcoma. *Oncogene*, **20**, 5736–5746.
3. Sorensen,P.H. *et al*. (2002) PAX3-FKHR and PAX7-FKHR gene fusions are prognostic indicators in alveolar rhabdomyosarcoma: a report from the children's oncology group. *J. Clin. Oncol.*, **20**, 2672–2679.
4. Fredericks,W.J. *et al*. (1995) The PAX3-FKHR fusion protein created by the t(2;13) translocation in alveolar rhabdomyosarcomas is a more potent transcriptional activator than PAX3. *Mol. Cell. Biol.*, **15**, 1522–1535.
5. Epstein,J.A. *et al*. (1995) Pax3 inhibits myogenic differentiation of cultured myoblast cells. *J. Biol. Chem.*, **270**, 11719–11722.
6. Scheidler,S. *et al*. (1996) The hybrid PAX3-FKHR fusion protein of alveolar rhabdomyosarcoma transforms fibroblasts in culture. *Proc. Natl Acad. Sci. USA*, **93**, 9805–9809.
7. Lam,P.Y. *et al*. (1999) The oncogenic potential of the Pax3-FKHR fusion protein requires the Pax3 homeodomain recognition helix but not the Pax3 paired-box DNA binding domain. *Mol. Cell. Biol.*, **19**, 594–601.
8. Anderson,M.J. *et al*. (2001) Embryonic expression of the tumor-associated PAX3-FKHR fusion protein interferes with the developmental functions of Pax3. *Proc. Natl Acad. Sci. USA*, **98**, 1589–1594.
9. Lagutina,I. *et al*. (2002) Pax3-FKHR knock-in mice show developmental aberrations but do not develop tumors. *Mol. Cell. Biol.*, **22**, 7204–7216.
10. Felix,C.A. *et al*. (1992) Frequency and diversity of p53 mutations in childhood rhabdomyosarcoma. *Cancer Res.*, **52**, 2243–2247.
11. Takahashi,Y. *et al*. (2004) Altered expression and molecular abnormalities of cell-cycle-regulatory proteins in rhabdomyosarcoma. *Mod. Pathol.*, **17**, 660–669.
12. Douglass,E.C. *et al*. (1987) A specific chromosomal abnormality in rhabdomyosarcoma. *Cytogenet. Cell Genet.*, **45**, 148–155.
13. Keller,C. *et al*. (2004) Alveolar rhabdomyosarcomas in conditional Pax3:Fkhr mice: cooperativity of Ink4a/ARF and Trp53 loss of function. *Genes Dev.*, **18**, 2614–2626.
14. Bois,P.R. *et al*. (2003) FKHR (FOXO1a) is required for myotube fusion of primary mouse myoblasts. *EMBO J.*, **22**, 1147–1157.
15. Buijs,A. *et al*. (2000) The MN1-TEL fusion protein, encoded by the translocation (12;22)(p13;q11) in myeloid leukemia, is a transcription factor with transforming activity. *Mol. Cell. Biol.*, **20**, 9281–9293.
16. Dick,J.E. *et al*. (1997) Assay of human stem cells by repopulation of NOD/SCID mice. *Stem Cells*, **15** (suppl. 1), 199–203;discussion 204–207.
17. Hannon,G.J. *et al*. (1999) MaRX: an approach to genetics in mammalian cells. *Science*, **283**, 1129–1130.
18. Tazi,J. *et al*. (2009) Alternative splicing and disease. *Biochim. Biophys. Acta*, **1792**, 14–26.
19. Caceres,J.F. *et al*. (2002) Alternative splicing: multiple control mechanisms and involvement in human disease. *Trends Genet.*, **18**, 186–193.
20. Faustino,N.A. *et al*. (2003) Pre-mRNA splicing and human disease. *Genes Dev.*, **17**, 419–437.
21. Dingwall,C. *et al*. (1988) The nucleoplasmin nuclear location sequence is larger and more complex than that of SV-40 large T antigen. *J. Cell Biol.*, **107**, 841–849.
22. Fischer,U. *et al*. (1995) The HIV-1 Rev activation domain is a nuclear export signal that accesses an export pathway used by specific cellular RNAs. *Cell*, **82**, 475–483.
23. Hanahan,D. *et al*. (2000) The hallmarks of cancer. *Cell*, **100**, 57–70.
24. Arnold,K. *et al*. (2006) The SWISS-MODEL workspace: a web-based environment for protein structure homology modelling. *Bioinformatics*, **22**, 195–201.
25. Zdobnov,E.M. *et al*. (2001) InterProScan—an integration platform for the signature-recognition methods in InterPro. *Bioinformatics*, **17**, 847–848.
26. Ben-Tovim Jones,L. *et al*. (2006) Use of micro array data via model-based classification in the study and prediction of survival from lung cancer. *Methods of Microarray Data Analysis*. Springer US, New York, NY, 163–173.

Received August 5, 2010; revised November 30, 2010; accepted December 11, 2010